Reflection of Thermoelastic Waves From the Insulated Surface of a Solid Half-Space With Time-Delay

Article *in* Journal of Heat Transfer · April 2020

DOI: 10.1115/1.4046924

4 authors, including:

Soumen De
University of Calcutta
84 PUBLICATIONS **230** CITATIONS
SEE PROFILE

Nantu Sarkar
University of Calcutta
67 PUBLICATIONS **714** CITATIONS
SEE PROFILE

Nihar Sarkar
Department of Mathematics,
City College,
Kolkata 700009, India
e-mail: nsmath.citycol@gmail.com

Soumen De
Department of Applied Mathematics,
University of Calcutta,
Kolkata 700 009, India
e-mail: soumenisi@gmail.com

Narayan Das
Department of Mathematics,
Government General Degree College,
Dantan-II,
Paschim Medinipur
West Bengal 721445, India
e-mail: narayandas8145@gmail.com

Nantu Sarkar[1]
Department of Applied Mathematics,
University of Calcutta,
Kolkata 700009, India
e-mail: nsarkarindian@gmail.com

Reflection of Thermoelastic Waves From the Insulated Surface of a Solid Half-Space With Time-Delay

This paper is devoted to study the reflection of thermoelastic plane waves from the thermally insulated stress-free boundary of a homogeneous, isotropic and thermally conducting elastic half-space. A new linear theory of generalized thermoelasticity under heat transfer with memory-dependent derivative (MDD) is employed to address this study. It has been found that three basic waves consisting of two sets of coupled longitudinal waves and one independent vertically shear-type wave may travel with distinct phase speeds. The formulae for various reflection coefficients and their respective energy ratios are determined in case of an incident coupled longitudinal elastic wave at the thermally insulated stress-free boundary of the medium. The results for the reflection coefficients and their respective energy ratios for various values of the angle of incidence are computed numerically and presented graphically for copper-like material and discussed.
[DOI: 10.1115/1.4046924]

1 Introduction

Scott Blair's model [1], which is basically a material model, includes a formula for memory phenomena in various disciplines. The model takes the form

$$ {}^{0}\mathcal{D}_t^{\alpha}\varepsilon(t) = \kappa\sigma(t) \tag{1} $$

where ${}^{0}\mathcal{D}_t^{\alpha}\varepsilon(t)$ denotes the fractional-order derivative, which depends on the strain history from 0 to t. For integral value of $\alpha = n$, ${}^{0}\mathcal{D}_t^{\alpha}\varepsilon(t) = d^n\varepsilon(t)/dt^n$, and $\kappa > 0$ is a constant. Equation (1) works not only in modeling viscoelastic materials but also in modeling biological kinetics with memory.

A fractional-order derivative is a generalization of an integer order derivative and integral. It originated from a letter of L'Hopital to Leibnitz in 1695 regarding the meaning of the half-order derivative. The kernel function of a fractional derivative is termed the memory function, but it does not replicate any physical process. Imprecise physical meaning has been a big obstacle that keeps fractional derivatives lagging far behind the integer-order calculus. There are several definitions of a fractional derivative. The Riemann–Liouville derivative is one of the most standard definitions

$$ {}^{0}\mathcal{D}_t^{\alpha}\varepsilon(t) = \frac{1}{\Gamma(n-\alpha)}\frac{d^n}{dt^n}\int_0^t \frac{\varepsilon(s)}{(t-s)^{1+\alpha-n}}ds, \quad n-1 \le \alpha < n $$

where $\Gamma(\cdot)$ is the Euler's gamma function and n is an integer. A memory process generally consists of two stages: the first is short, with permanent retention at the beginning, and it cannot be neglected in general, and the second is governed by the fractional model Eq. (1). The critical point between the fresh stage and the working stage is usually not the origin. This is quite different from the traditional fractional models of one stage. The key point is that the order of a fractional derivative is an index of memory. The dimensionless form of the solution of Eq. (1) is

$$ E(\eta) = \eta^{\alpha} - (\eta-1)^{\alpha} \tag{2} $$

where $\eta = t/t_M$ and $E(\eta) = \varepsilon(t)/\varepsilon_M$, where ε_M is the strain at the end of time of creeping $t = t_M$. Equation (2) reveals that $E(\eta)$ increases with an increase in α. The higher the value of the index α, the slower is the forgetting during the process. In particular, at $\alpha = 0$, $E = 0$, meaning that "nothing is memorized," and $E = 1$ for $\alpha = 1$, which means that "nothing is forgotten." Therefore, the fractional order α is basically termed as the index of the memory effect.

For a standard creep and recovery process, the specimen is usually loaded under a constant stress $\sigma(t) = \sigma_0$ from 0 to t_M, and the load is removed at the instant $t = t_M$, then $\sigma(t) = 0$ for $t \ge t_M$. If $H(t)$ is the Heaviside function, Eq. (1) takes the following form:

$$ {}^{0}\mathcal{D}_t^{\alpha}\varepsilon(t) = \kappa\sigma_0(H(t) - H(t-t_M)) $$

where ${}^{0}\mathcal{D}_t^{\alpha}\varepsilon(t)$ is the Riemann–Liouville fractional-order derivative with zero initial condition. The superposition method gives the solution of the above equation as follows:

$$ \varepsilon(t) = \frac{\kappa\sigma_0}{\Gamma(1+\alpha)}\left[t^{\alpha}H(t) - (t-t_M)^{\alpha}H(t-t_M)\right] $$

This is in agreement with the early observation of the behavior of some viscoelastic materials.

The nonintegral (fractional)-order derivatives and the fractional differential equations have gained considerably more attention in the fields of applied sciences and various engineering disciplines [1]. Diethelm [2] incorporated a kernel function and modified a Caputo-type fractional-order derivative as

$$ \mathcal{D}_a^{\alpha}f(t) = \int_a^t k_{\alpha}(t-\xi)f^{(m)}(\xi)d\xi $$

[1]Corresponding author.

Contributed by the Heat Transfer Division of ASME for publication in the Journal of Heat Transfer. Manuscript received February 11, 2019; final manuscript received March 28, 2020; published online June 12, 2020. Editor: Portonovo S. Ayyaswamy.

where $k_\alpha(t-\xi)$ is the kernel function and $f^{(m)}$ is the mth order derivative. In applications, $k_\alpha(t-\xi)$ takes some specific form, e.g.,

$$k_\alpha(t-\xi)=\frac{(t-\xi)^{m-\alpha-1}}{\Gamma(m-\alpha)}$$

Wang and Li [3] proposed another form of the fractional derivative with arbitrary kernel $K(t-\xi)$ (can be chosen freely) over a slipping interval $[t-\tau,t]$ as follows:

$$\mathcal{D}_\tau^{(1)}f(t)=\frac{1}{\tau}\int_{t-\tau}^{t}K(t-\xi)f'(\xi)d\xi \tag{3}$$

where $\tau\,(>0)$ is called the delay time, which can also be chosen freely. The preceding modifications of fractional-ordered derivatives are termed memory-dependent derivatives (MDDs). In general, the mth order memory-dependent derivative of a differentiable function $f(t)$ relative to the time delay, $a>0$ is defined as

$$\mathcal{D}_a^{(m)}f(t)=\frac{1}{\tau}\int_{t-a}^{t}K(t,\xi)f^{(m)}(\xi)d\xi$$

where the time delay a denotes the memory scale, and the kernel function $K(t.\xi)$ must be a differentiable function with respect to its arguments. The kernel function and the memory scales must be chosen in such a way that they are compatible with the physical problem, so this type of derivative provides more possibilities to capture the material response [3]. Generally, the memory effect needs weight $0\le K(t-\xi)\le 1$ for $\xi\in[t-\tau,t]$ so that the magnitude of $D_\tau f(t)$ is usually smaller than that of the common derivative $f'(t)$. Simply the right-hand side of Eq. (3) is a weighted mean of $f'(t)$. As $\xi\in[t-\tau,t]$, one can easily understand that the function $f(\xi)$ takes value from different points on the time interval $[t-\tau,t]$. Considering our present time as t, we can say $[t-\tau,t)$ is the past time interval. Thus, we conclude the main feature of MDD, that is the functional value in real-time depends on the past time also. That is why D_τ is called the nonlocal operator, whereas integer order derivative (or integration) is a local operator (i.e., it does not depend on the past time). The kernel function $K(t-\xi)$ can be chosen freely, such as $1,[1-(t-\xi)],[1-(t-\xi)/\tau]^p$ for any positive real number p, which may be more practical [3]. They are a monotonic increasing function from 0 to 1 in the interval $[t-\tau,t]$. According to the nature of the problem, one can select a suitable kernel function of his/her choice.

From the Maxwell–Cattaneo theory [4] to Green-Naghdi generalized thermoelasticity models [5], it is well established that the thermal memory has a significant role in the theory of generalized thermoelasticity [6–9]. In the 21st century, memory components have been introduced in terms of fractional-order derivatives in numerous forms, see Refs. [10–12] for details. In these fractional models of modified heat flux laws, the memory response is described by the fractional index parameter. The MDD were first incorporated in the Fourier's law of heat conduction [4], a new hyperbolic-type heat conduction equation, by Wang and Li [3]. This new generalization of hyperbolic-type heat conduction models is accepted as the modified heat conduction law with measuring memory. Following the work of Wang and Li [3], Yu et al. [13] developed a novel generalized thermoelasticity model based on generalized Fourier's law of heat conduction with MDD by introducing

$$(1+\tau\mathcal{D}_a)q_i=-K_T\Theta_{,i} \tag{4}$$

where $D_af(t)=D_a^{(1)}f(t)$. They also studied slim strip problem of thermoelastic medium under this new theory. Later, Ezzat et al. [14–16] introduced the first-order MDD, instead of fractional calculus, into the rate of heat flux in the Lord-Shulman (LS) theory [6] of generalized thermoelasticity to denote memory dependence as

$$(1+\tau D_\tau)q_i=-K_T\Theta_{,i} \tag{5}$$

where τ is introduced as the delay time parameter, q_i are the heat flux components, $\Theta=T-T_0$ is the temperature increment above the uniform reference temperature T_0 of the medium, T is the absolute temperature of the medium, and K_T is the thermal conductivity. Above equation has more clear physical meaning. Equations (4) and (5) provide the following advantages compared with the aforementioned amendments of Fourier's law by using fractional derivatives: (i) the influence of memory dependency claims its superiority in terms of memory scale parameter; (ii) in a limiting sense, this simplification develops the Lord-Shulman model of generalized thermoelasticity and (iii) because the kernel function and the memory scale parameters may be chosen subjectively, it is more malleable in many practical applications. Several physical problems in the context of this new theory of generalized thermoelasticity with MDD have been reported in the literatures [14–19].

Wave propagation and wave reflection phenomena are applicable in various fields like geophysical exploration, mineral and oil exploration, and seismology. The body wave propagation in thermoelastic solids is applicable in various fields of engineering. Several problems on plane harmonic wave propagation in coupled and generalized thermoelasticities have been investigated by many authors during the last five decades. Some of the notable among them are found in the literatures [20–31]. Recently, Li et al. [32] investigated the reflection and transmission of elastic waves at an interface with consideration of couple stress and thermal wave effects. Sarkar and Tomar [33] studied plane waves in nonlocal thermoelastic solid with voids. Waves in dual-phase-lag thermoelastic materials with voids based on Eringen's nonlocal elasticity were discussed by Mondal et al. [34]. Das et al. [35] solved the problem of reflection of thermoelastic wave from an insulated and isothermal stress-free boundary of a solid half space without energy dissipation. They preferred to investigate the problem by specifying the angles of incidence and reflections with the normal to the half-space. Sarkar et al. [36,37] addressed the reflection of thermoelastic waves from the boundary of a solid half-space under memory-dependent heat transfer.

In the present contribution, the reflection phenomena of coupled thermoelastic plane waves from the thermally insulated stress-free boundary of a homogeneous, isotropic and thermally conducting solid half-space is addressed in the context of the generalized thermoelasticity with MDD [15]. It has been observed that three basic waves consisting of two sets of coupled dilatational thermoelastic waves and one independent shear-type wave may travel with distinct phase speeds. The formulae for various reflection coefficients and their respective energy ratios are determined due to the incidence of a coupled dilatational elastic wave at the thermally insulated stress-free boundary of the medium. The numerical results for the reflection coefficients and their respective energy ratios for various values of the angle of incidence are illustrated graphically for copper like material to highlight the effect of time-delay, kernel function, Poison ratio, and the thermomechanical coupling parameter. The phase speeds and the attenuation coefficients are also computed numerically and plotted graphically to study the effect of the various parameters of interest.

2 Governing Equations

Following Ezzat et al. [14], the basic governing equations of the generalized thermoelasticity with memory-dependent derivative heat transfer for a homogeneous, isotropic, and thermally conducting elastic solid in the general Cartesian coordinates system are (in absence of heat sources and body forces)

$$\tau_{ij}=2\mu e_{ij}+(\lambda e-\gamma\Theta)\delta_{ij} \tag{6}$$

$$\mu u_{i,jj} + (\lambda + \mu) u_{j,ij} - \gamma \Theta_{,i} = \rho \ddot{u}_i \tag{7}$$

$$K_T \Theta_{,ii} = (1 + \tau D_\tau)(\rho C_E \dot{\Theta} + \gamma T_0 \dot{e}) \tag{8}$$

where $i, j = 1, 2, 3$, $e_{ij} = (u_{i,j} + u_{j,i})/2$. Here, τ_{ij} are the components of the stress tensor, e_{ij} are the components the infinitesimal strain tensor in linear elasticity, $e = u_{i,i}$ is the cubical dilatation, u_i are the displacement components, λ, μ are Lamé constants, ρ is the mass density, C_E is the specific heat at the constant strain, $\gamma = (3\lambda + 2\mu)\alpha_T$ is the thermoelastic coupling parameter, and α_T is the coefficient of volume expansion.

Using the definition (3) of memory-dependent derivative, Eq. (8) can also be rewritten as

$$K_T \Theta_{,ii} = (\rho C_E \dot{\Theta} + \gamma T_0 \dot{e}) + \int_{t-\tau}^{t} K(t - \xi)(\rho C_E \Theta_{,\xi\xi} + \gamma T_0 e_{,\xi\xi}) d\xi \tag{9}$$

Equation (8) or (9) is the generalized heat conduction equation with memory-dependent derivative having τ as the time-delay parameter. The dynamic coupled theory of heat conduction law follows as the limit case when $\tau \to 0$. Note that, in the above equations, a comma followed by a suffix denotes *spatial derivative* and a *superposed dot* stands for time differentiation.

3 Formulation of the Problem

We consider a linear, homogeneous, and isotropic thermally conducting elastic medium occupying the half-space

$$\Omega = \{(x, y, z) : -\infty < x, y < \infty, 0 \le z < \infty\}$$

Let the origin O of the rectangular Cartesian coordinate system $Oxyz$ be fixed at a point on the boundary $z = 0$ with z-axis directed normally inside the medium Ω and x-axis is directed along the horizontal direction. The y-axis is taken in the direction of the line of intersection of the plane wavefront with the plane surface. If we restrict our analysis to a plane strain problem parallel to the xz-plane, then all the field variables may be taken as functions of x, z, and t only. Hence, the displacement components are

$$u_1 = u(x, z, t), \quad u_2 = v(x, z, t) = 0, \quad u_3 = w(x, z, t)$$

Then Eqs. (6)–(8) reduce to

$$\tau_{xx} = 2\mu u_{,x} + \lambda e - \gamma \Theta \tag{10}$$

$$\tau_{zz} = 2\mu w_{,z} + \lambda e - \gamma \Theta \tag{11}$$

$$\tau_{xz} = \mu(u_{,z} + w_{,x}) \tag{12}$$

$$\mu \nabla^2 u + (\lambda + \mu) e_{,x} - \gamma \Theta_{,x} = \rho \ddot{u} \tag{13}$$

$$\mu \nabla^2 w + (\lambda + \mu) e_{,z} - \gamma \Theta_{,z} = \rho \ddot{w} \tag{14}$$

$$K_T \nabla^2 \Theta = (1 + \tau D_\tau)(\rho C_E \dot{\Theta} + \gamma T_0 \dot{e}) \tag{15}$$

In this study, we shall deal with the following kernel function [14]:

$$K(t - \xi) = 1 - \frac{2b}{\tau}(t - \xi) + \frac{a^2 (t - \xi)^2}{\tau^2} = \begin{cases} 1 & \text{if } a = b = 0 \\ 1 - \left(\dfrac{t - \xi}{\tau}\right) & \text{if } a = 0, b = \dfrac{1}{2} \\ 1 - (t - \xi) & \text{if } a = 0, b = \dfrac{\tau}{2} \\ \left(1 - \dfrac{t - \xi}{\tau}\right)^2 & \text{if } a = b = 1 \end{cases} \tag{16}$$

where a and b are constants.

To transform the above equations in nondimensional forms, we define the following nondimensional variables

$$(x', z') = C_L \eta(x, z), \quad (u', w') = C_L \eta(u, w), \quad t' = C_L^2 \eta t, \quad \Theta' = \frac{\gamma \Theta}{\rho C_L^2}, \quad \sigma'_{ij} = \frac{\sigma_{ij}}{\rho C_L^2}$$

where $C_L^2 = (\lambda + 2\mu)/\rho$ is the speed of classical longitudinal (dilatational) wave and $\eta = \rho C_E / K_T$ is the thermal viscosity. Introducing the above parameters in Eqs. (10)–(15) and suppressing the primes for convenience, we obtain

$$\tau_{xx} = 2\beta u_{,x} + (1 - 2\beta) e - \Theta \tag{17}$$

$$\tau_{zz} = 2\beta w_{,z} + (1 - 2\beta) e - \Theta \tag{18}$$

$$\tau_{xz} = \beta(u_{,z} + w_{,x}) \tag{19}$$

$$\beta \nabla^2 u + (1 - \beta) e_{,x} - \Theta_{,x} = \ddot{u} \tag{20}$$

$$\beta \nabla^2 w + (1 - \beta) e_{,z} - \Theta_{,z} = \ddot{w} \tag{21}$$

$$\nabla^2 \Theta = (1 + \tau D_\tau)(\dot{\Theta} + \varepsilon \dot{e}) \tag{22}$$

where $\nabla^2 \equiv \partial^2/\partial x^2 + \partial^2/\partial z^2$, $\beta = \mu/(\lambda + 2\mu) = (1 - 2\sigma)/[2(1 - \sigma)]$ is the ratio of the classical shear wave speed to the classical longitudinal wave speed, σ is the Poison's ratio, and $\varepsilon = \gamma^2 T_0/[\rho C_E(\lambda + 2\mu)]$ is defined as the dimensionless *thermoelastic coupling constant*.

Introducing the displacement potentials ϕ (corresponds to dilatational wave) and ψ (corresponds to shear-type wave) through the Helmholtz vector decomposition technique as

$$u = \frac{\partial \phi}{\partial x} - \frac{\partial \psi}{\partial z}, \qquad w = \frac{\partial \phi}{\partial z} + \frac{\partial \psi}{\partial x} \tag{23}$$

and substituting these into Eqs. (20)–(22), we obtain

$$\nabla^2 \phi - \ddot{\phi} - \Theta = 0 \tag{24}$$

$$\beta \nabla^2 \psi - \ddot{\psi} = 0 \tag{25}$$

$$\nabla^2 \Theta = (1 + \tau D_\tau)(\dot{\Theta} + \varepsilon \nabla^2 \dot{\phi}) \tag{26}$$

Equations (24) and (26) show that the thermal field Θ is coupled with the potential ϕ and so creates two quasi-thermal-elastic waves, one of them is called quasi-elastic wave (qP-wave) while the other one is called quasi-thermal wave (qT-wave). Equation (25) creates one independent vertically polarized shear-type wave (SV-type wave).

4 Dispersion Equation and Its Solution

For a harmonic plane wave propagating in the direction where the wave normal vector lies in the xz-lane making an angle θ_0 with the positive z-axis, the solutions of Eqs. (24)–(26) may be assumed as

$$(\phi, \Theta, \psi) = (A_\phi, A_\Theta, A_\psi) \exp\{\iota k(x \sin\theta_0 - z \cos\theta_0) - \iota \omega t\} \tag{27}$$

where A_ϕ, A_Θ, A_ψ are the constants (possible complex) representing the coefficients of the wave amplitudes, $\iota = \sqrt{-1}$, k is the wavenumber to be determined, and ω is the assigned real angular frequency.

Substituting Eq. (27) into Eqs. (24)–(26), we get

$$(k^2 - \omega^2) A_\phi + A_\Theta = 0 \tag{28}$$

$$\left(k^2 - \frac{\omega^2}{\beta}\right) A_\psi = 0 \tag{29}$$

$$\iota\varepsilon\omega(1+G)k^2 A_\phi + [k^2 - \iota\omega(1+G)]A_\Theta = 0 \tag{30}$$

where Eq. (16) gives

$$G \equiv G(\tau,\omega) = \frac{1}{\tau^2\omega^2}[\exp(\iota\tau\omega)\{2a^2 - \tau^2\omega^2(a^2 - 2b + 1) - 2\iota\tau\omega(a^2 - b^2)\} - 2\iota b\tau\omega - 2a^2 + \tau^2\omega^2]$$

The condition for the existence of nonvanishing solution for A_ϕ and A_Θ of the system of Eqs. (28) and (30) yields the following dispersion relation:

$$k^4 - L_1 k^2 + L_2 = 0 \tag{31}$$

where $L_1 = \iota\omega(1+G)(1+\varepsilon) + \omega^2$, $L_2 = i\omega^3(1+G)$.

The quadratic Eq. (31) in k^2 is the general dispersion relation for wave propagation in thermoelastic solid with MDD. Clearly, the coefficients L_1 and L_2 are complex for $\omega > 0$. The two roots of Eq. (31) and the only root of Eq. (29) are given by

$$k_{2,1}^2 = \frac{1}{2}\left[L_1 \pm \sqrt{L_1^2 - 4L_2}\right], \quad k_3^2 = \frac{\omega^2}{\beta}$$

Here, k_1^2 corresponds to "–" sign and k_2^2 corresponds to "+" sign. Out of the four roots $\pm k_{1,2}$, we consider those two roots only for which $\Im(k_{1,2}) \geq 0$ for the waves to be physically realistic [37]. These two complex wavenumbers give us two distinct types of attenuated and dispersive coupled dilatational waves: one quasi-elastic wave (qP-wave) and one quasi-thermal wave (qT-wave). Besides, since the wavenumbers of both the qP- and qT-wave are complex, they are inhomogeneous waves. The phase speeds V_j and attenuation coefficients Q_j $(j = 1, 2)$ of the qP- and qT-waves can be obtained from the formulae [38]

$$V_j = \frac{\omega}{\Re(k_j)}, \quad Q_j = \Im(k_j) \tag{32}$$

where $\Re(\cdot)$ and $\Im(\cdot)$ denote the real and imaginary part, respectively.

In case of *uncoupled thermoelasticity* $(\varepsilon = 0)$, we find

$$V_1 = 1, \quad V_2 = \frac{\sqrt{\omega}}{\Re[\iota(1+G)]^{\frac{1}{2}}}$$

Thus, for the present problem $(\varepsilon \neq 0)$, we conclude that while V_1 represents the speed of qP-wave, V_2 the speed of qT-wave (according to our consideration of the sign of k_1^2 and k_2^2). In case of $\varepsilon \neq 0$, the qP-wave and qT-wave are coupled dilatational-thermal wave and the coupling is measured by the following amplitudes ratios:

$$\left(\frac{A_\Theta}{A_\phi}\right)_j = \left(\omega^2 - k_j^2\right) = \frac{\varepsilon\omega(1+G)k_j^2}{\left[\omega(1+G) + \iota k_j^2\right]} = \zeta_j \quad (j = 1, 2)$$

Equation (25) shows that there exists one SV-type wave of wave number k_3, which remains unaffected by the thermal wave. The phase speed V_3 and the attenuation coefficient Q_3 of this wave are

$$V_3 = \sqrt{\beta}, \quad Q_3 = 0$$

which tell us that the SV-type wave is nondispersive and experience no attenuation.

4.1 Perturbation Solution of Dispersive Waves. The perturbation method has been widely used (Nayfeh and Nemat-Nasser [20], Agarwal [21], Roychoudhuri [22,25], Sharma et al. [29]) to study the wave propagation problems in classical (coupled) and nonclassical (generalized) thermoelastic continua. Here, our aim is to derive the perturbation solution of the instant problem in this section. The secular Eq. (31) can also be rewritten as

$$f(k^2) - \varepsilon g(k^2) = 0 \tag{33}$$

where

$$f(k^2) = k^4 - k^2[\iota\omega(1+G) + \omega^2] + i\omega^3(1+G),$$
$$g(k^2) = \iota\omega(1+G)k^2$$

For most of the materials, the thermo-mechanical coupling parameter ε is very small and therefore, we develop series expansions in terms of ε for the roots k_j^2 $(j = 1, 2)$ of the Eq. (33) in order to explore the effect of various interacting fields on the waves. Thus, for $\varepsilon \ll 1$, we obtain

$$k_1^2(\varepsilon) = \omega^2\left[1 - \frac{(1+G)}{(1+G+\iota\omega)}\varepsilon + \cdots\right],$$
$$k_2^2(\varepsilon) = \iota\omega(1+G)\left[1 + \frac{(1+G)}{(1+G+\iota\omega)}\varepsilon + \cdots\right] \tag{34}$$

Using the perturbation solution (34) into Eq. (32), the phase velocities and attenuation coefficients can be obtained for small ε.

5 Reflection Phenomenon of Thermoelastic Waves

In view of the results of Secs. 4–6, consider an incident qP-wave propagating obliquely toward the surface $z = 0$ of the thermoelastic medium as shown in Fig. 1. Assuming that the radiation in vacuum is neglected, when it impinges the boundary $z = 0$, three reflected waves in the medium Ω are created. Suppose the reflected qP-, qT- and SV-type waves make angles θ_1, θ_2, and θ_3, respectively, with the positive z-axis. Then the complete structures of the wave fields consisting of the incident and the reflected waves in the medium Ω may be written as

$$\phi = A_0 \exp\{\iota k_1(x\sin\theta_0 - z\cos\theta_0) - \iota\omega t\} + \sum_{j=1}^{2} A_j \exp\{\iota k_j(x\sin\theta_j + z\cos\theta_j) - \iota\omega t\} \tag{35}$$

$$\Theta = \zeta_1 A_0 \exp\{\iota k_1(x\sin\theta_0 - z\cos\theta_0) - \iota\omega t\} + \sum_{j=1}^{2} \zeta_j A_j \exp\{\iota k_j(x\sin\theta_j + z\cos\theta_j) - \iota\omega t\} \tag{36}$$

$$\psi = B_1 \exp\{\iota k_3(x\sin\theta_3 + z\cos\theta_3) - \iota\omega t\} \tag{37}$$

where A_1, A_2, and B_1 represent the coefficients of amplitudes of the reflected qP-, qT- and SV-waves, respectively, and A_0

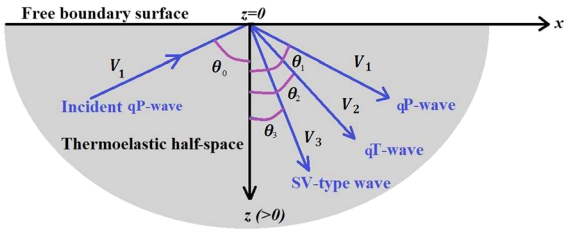

Fig. 1 Schematic of the present problem: incident and reflected thermoelastic waves at the surface $z = 0$

represents the amplitude coefficient of the incident qP-wave with phase speed V_1. The reflection coefficients are defined as the amplitude ratios of the reflected wave to the incident wave and are determined by the well-defined boundary conditions on the surface $z=0$. In the present problem, we consider the surface $z=0$ as stress-free and thermally insulated. Mathematically, these conditions can be written as

$$\tau_{zz} = \tau_{zx} = 0, \quad \frac{\partial \Theta}{\partial z} = 0 \ \text{ at } \ z = 0 \tag{38}$$

In terms of potential functions, the stress-free conditions in Eqs. (18) and (19) can be written as

$$(\phi_{,xx} + \phi_{,zz}) + 2\beta(\psi_{,xz} - \phi_{,xx}) - \Theta = 0 \tag{39}$$

$$2\phi_{,xz} + \psi_{,xx} - \psi_{,zz} = 0 \tag{40}$$

In order to satisfy the above boundary conditions at $z=0$, the following relations between the angle of the incident wave and the angles of the reflected waves need to be hold on $z=0$:

$$k_1 \sin\theta_0 = k_1 \sin\theta_1 = k_2 \sin\theta_2 = k_3 \sin\theta_3 \tag{41}$$

Relation (41) can also be written in the form

$$\theta_0 = \theta_1 \quad \text{and} \quad \frac{\sin\theta_0}{V_1} = \frac{\sin\theta_2}{V_2} = \frac{\sin\theta_3}{V_3} \tag{42}$$

which is often refereed as *extended Snell's law*.

Substituting Eqs. (35)–(37) into the boundary conditions (38)–(40) and using the relation (41) or (42), the following system of equations for the reflection coefficients $X_1 = A_1/A_0$, $X_2 = A_2/A_0$, $X_3 = B_1/A_0$ is obtained:

$$\begin{bmatrix} a_{11} & a_{12} & a_{13} \\ a_{21} & a_{22} & a_{23} \\ a_{31} & a_{32} & 0 \end{bmatrix} \begin{bmatrix} X_1 \\ X_2 \\ X_3 \end{bmatrix} = \begin{bmatrix} -a_{11} \\ a_{21} \\ a_{31} \end{bmatrix} \tag{43}$$

where

$$a_{11} = \omega^2 - 2\beta k_1^2 \sin^2\theta_0, \quad a_{12} = \omega^2 - 2\beta k_2^2 \sin^2\theta_2,$$
$$a_{13} = \omega^2 \sin 2\theta_3$$
$$a_{21} = k_1^2 \sin 2\theta_0, \quad a_{22} = k_2^2 \sin 2\theta_2, \quad a_{23} = -k_3^2 \cos 2\theta_3$$
$$a_{31} = \zeta_1 k_1 \cos\theta_1, \quad a_{32} = \zeta_2 k_2 \cos\theta_2$$

After solving the system (43), we obtain the reflection coefficients in explicit forms as follows:

$$X_1 = \frac{\beta^2\zeta_2 k_2 k_3^2 \sin(4\theta_0)\cos(\theta_2)}{-\zeta_1 k_1 \cos(\theta_1)\left(\omega^2\cos(2\theta_0) + 2\beta^2 k_2^2 \sin(2\theta_0 - \theta_2)\sin(\theta_2)\right) + 2\beta^2\zeta_2 k_1^2 k_2 \sin(2\theta_0 - \theta_1)\sin(\theta_1)\cos(\theta_2) + \zeta_2 k_2 \omega^2 \cos(2\theta_0)\cos(\theta_2)}$$

$$X_2 = \frac{\beta^2\zeta_1 k_1 k_3^2 \sin(4\theta_0)\cos(\theta_1)}{\zeta_1 k_1 \cos(\theta_1)\left(\omega^2\cos(2\theta_0) + 2\beta^2 k_2^2 \sin(2\theta_0 - \theta_2)\sin(\theta_2)\right) - 2\beta^2\zeta_2 k_1^2 k_2 \sin(2\theta_0 - \theta_1)\sin(\theta_1)\cos(\theta_2) + \zeta_2 k_2 \omega^2 (-\cos(2\theta_0))\cos(\theta_2)}$$

$$X_3 = \frac{\zeta_1 k_1 \cos(\theta_1)\left(2\beta^2 k_2^2 \sin(\theta_2)\sin(2\theta_0 + \theta_2) - \omega^2\cos(2\theta_0)\right) - 2\beta^2\zeta_2 k_1^2 k_2 \sin(\theta_1)\sin(2\theta_0 + \theta_1)\cos(\theta_2) + \zeta_2 k_2 \omega^2 \cos(2\theta_0)\cos(\theta_2)}{\zeta_1 k_1 \cos(\theta_1)\left(\omega^2\cos(2\theta_0) + 2\beta^2 k_2^2 \sin(2\theta_0 - \theta_2)\sin(\theta_2)\right) - 2\beta^2\zeta_2 k_1^2 k_2 \sin(2\theta_0 - \theta_1)\sin(\theta_1)\cos(\theta_2) + \zeta_2 k_2 \omega^2 (-\cos(2\theta_0))\cos(\theta_2)}$$

The above expressions show that the reflection coefficients depend on the material properties of the medium Ω, angle of incidence θ_0 and the time-delay parameter τ.

It is to be noted that, for uncoupled thermoelasticity, we put $\varepsilon = 0$ which gives $\zeta_j = 0\,(j = 1, 2)$. Hence, there will be no reflected qT-wave in uncoupled thermoelasticity. Consequently, $X_2 = 0$ at all angle of incidence θ_0.

6 Energy Partitioning: Energy Ratios of the Reflected Waves Due to an Incident qP-Wave

In order to physically justify the analytic expressions of the amplitude ratios in the present problem, we must need to verify the energy balance law at the boundary surface $z=0$. Let us consider the energy partition between the various reflected waves at a surface element of unit area. Following Ref. [38], the rate of energy transmission, say P^* per unit area at a free surface of a thermoelastic solid, is given by

$$P^* = \tau_{zz}\dot{w} + \tau_{zx}\dot{u} \tag{44}$$

Note that here the contribution of thermal energy as well as the interaction energy is negligibly so small compared to the other energy terms. Also, even if these energies are accounted in Eq. (44), these do not change the results qualitatively. However, some physical situations may arise where the contribution of thermal energy as well as the interaction energy is comparable to the other energy and in that case it is essential to include these energies in Eq. (44) (cf. Li et al. [39]).

The energy ratio E_j corresponding to the j-th reflected wave at $z=0$ is obtained by calculating the ratio of "P^* for the reflected wave" to "P^* for the incident wave," i.e.,

$$E_j = \frac{P^*\,(\text{reflected wave})}{P^*\,(\text{incident wave})}, \quad j = 1, 2, 3 \tag{45}$$

Substituting Eqs. (35)–(37) into Eq. (44) through the Eqs. (18), (19), and (23), we obtained P^* for various incident and reflected waves. Hence, the analytical expressions of the energy ratios E_1, E_2, and E_3 for the reflected qP-, qT- and SV-type waves, respectively, due to the incident qP-wave can be calculated using Eq. (45) as

$$E_1 = -X_1^2, \quad E_2 = -\frac{\tan\theta_0}{\tan\theta_2}X_2^2, \quad E_3 = -\frac{\tan\theta_0}{\tan\theta_3}X_3^2,$$
$$0\,\text{deg} < \theta_0 < 90\,\text{deg}$$

We also observe that the energy ratios depend on the elastic properties of the medium, angle of incidence, time-delay parameter, and the reflection coefficients. Since surface waves are not involved in energy conservation, the conservation of energy at the boundary surface $z=0$ may be expressed as $|E_1 + E_2 + E_3| \approx 1$.

7 Numerical Results and Discussions

In this section, we perform some numerical results in order to illustrate the analytical results calculated in Sec. 7 for the

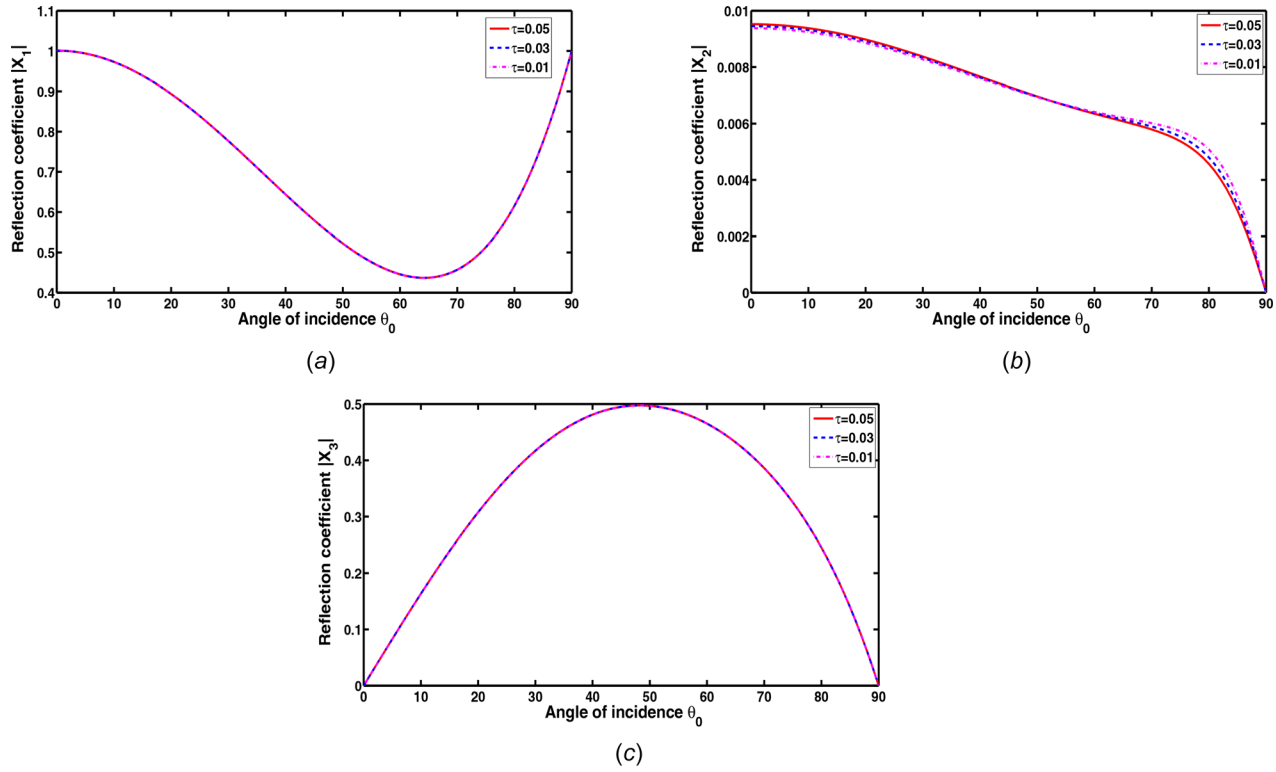

Fig. 2 (*a*)–(*c*) Variation of $|X_j|$ versus θ_0 for different τ when $K(t-\xi) = 1-(t-\xi)$

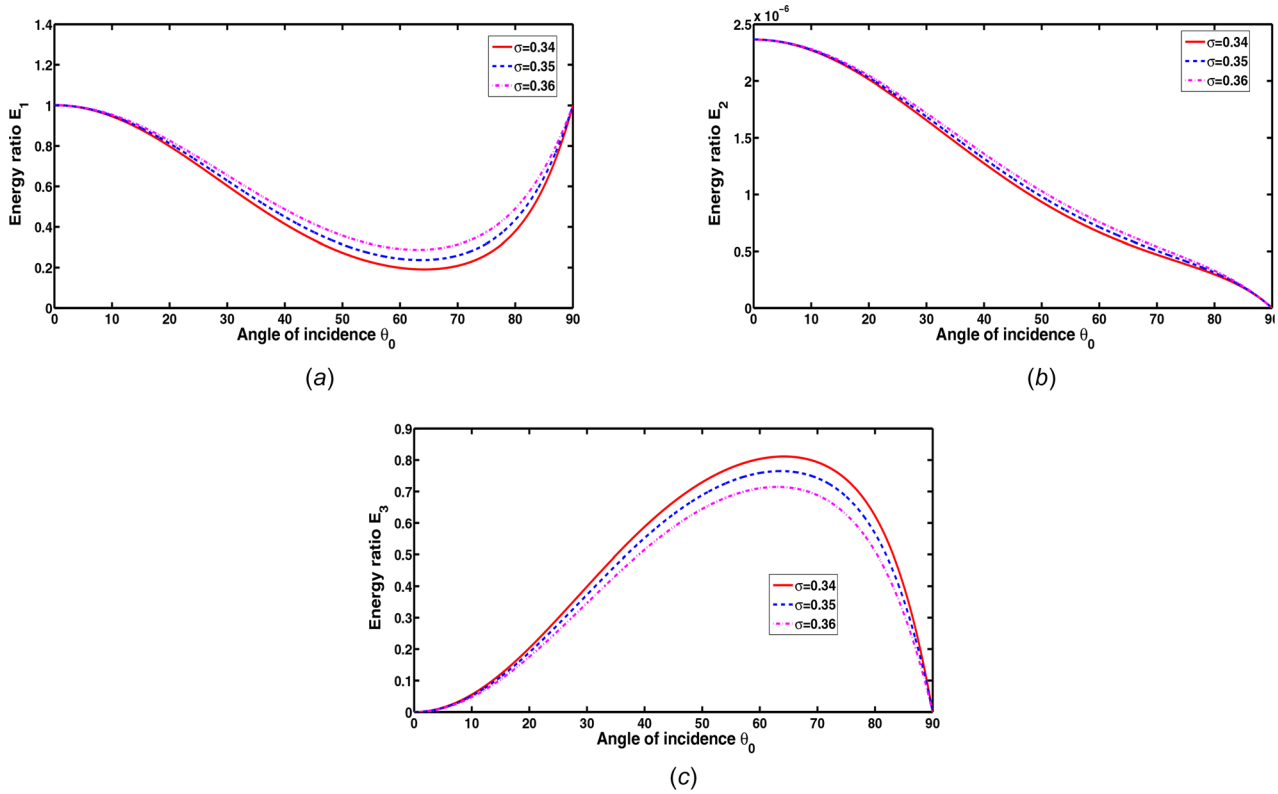

Fig. 3 (*a*)–(*c*) Variation of $|X_j|$ versus θ_0 for different $K(t, \xi)$ when $\tau = 0.05$

reflection coefficients, energy ratios, phase speeds, and the attenuation coefficients. For this purpose, copper-like material is modeled as the thermoelastic material for which the following values of the different physical constants are borrowed from Ref. [36].

Using MATLAB software, the variations of the absolute values of the reflection coefficients $X_j\,(j = 1, 2, 3)$ with respect to the angle of incidence θ_0 are presented graphically through Figs. 2–5 and Supplementary Figs. 1–5 are available in the

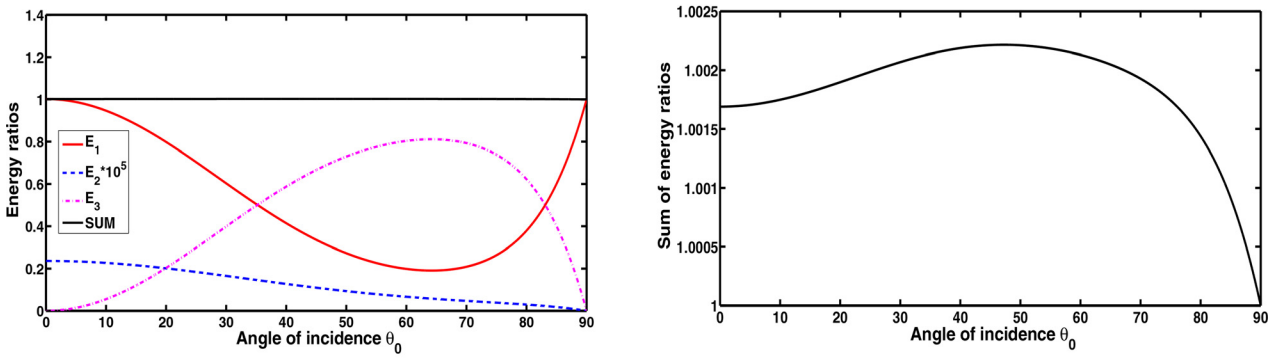

(*a*) (*b*)

Fig. 4 (*a*)–(*b*) Variations of $|X_j|$ versus θ_0 for different σ when $\tau = 0.05$, $K(t-\xi) = 1-(t-\xi)/\tau$

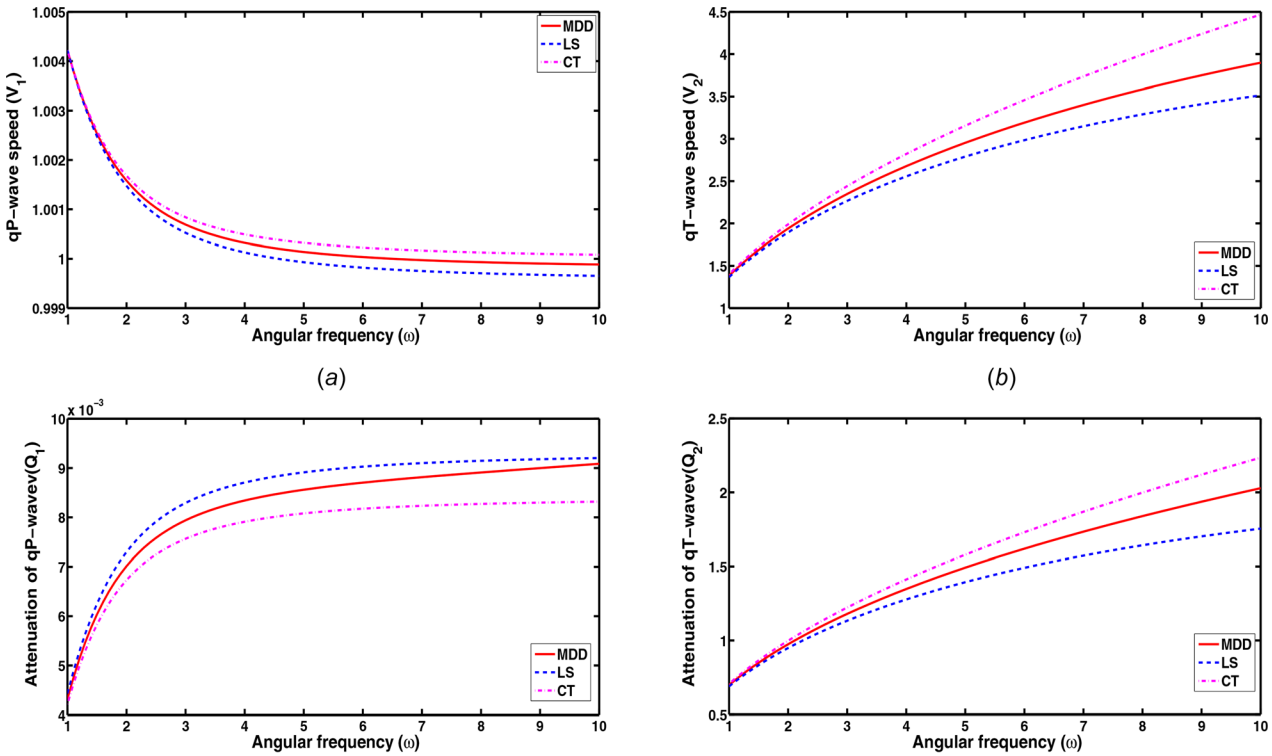

(*a*) (*b*) (*c*) (*d*)

Fig. 5 (*a*)–(*d*) Variations of $|X_j|$ versus θ_0 for different ε when $\tau = 0.05$, $K(t,\xi) = (1-(t-\xi)/\tau)^2$

Supplemental Materials on the ASME Digital Collection for the incident qP-wave. Using the numerical values in the Table 1, numerically computed values of the reflection coefficients, energy ratios, phase speeds, and the attenuation coefficients are plotted with θ_0 for the range $0\,\text{deg} \le \theta_0 \le 90\,\text{deg}$ in some different cases.

In this work, we devoted to investigate the reflection phenomena of thermoelastic waves at a stress-free isothermal boundary by considering the memory dependence for heat transfer with thermal relaxation. The key parameters are the time-delay factor and the kernel function of the MDD and the thermoelastic coupling parameter ε. As described in the paper, the most advantage of the generalized thermoelastic model based on heat transfer with MDD is the free choosing of the delay time factor and the kernel function, which makes it flexible in applications. In the obtained numerical results, we demonstrated the different effects of the time-delay factor, kernel function, Poison's ratio, and thermoelastic coupling parameter on the variations of the reflection coefficients and the energy ratios of the reflected qP-, qT- and SV-type wave as follows.

Figure 2 shows the reflection coefficients ($|X_j|$) profiles for three values of the time-delay parameter τ $(0.05, 0.03, 0.01)$ for a fixed kernel $K(t,\xi) = 1-(t-\xi)$. It is evident from Fig. 2(*a*) that the reflection coefficient $|X_1|$ of the reflected qP-wave decreases for $0\,\text{deg} \le \theta_0 \le 65\,\text{deg}$ and then increases in $65\,\text{deg} \le \theta_0 \le 90\,\text{deg}$ to reach unity for all values of τ. The maximum of $|X_1|$ is unity which occurs at $\theta_0 = 0\,\text{deg}$ and $90\,\text{deg}$. Figure 2(*b*) exhibits that the reflection coefficient $|X_2|$ of the reflected qT-wave attains its maximum at $\theta_0 = 0\,\text{deg}$ and then it decreases continuously with the increasing θ_0 until vanishes at $\theta_0 = 90\,\text{deg}$. From Fig. 2(*c*), we see that the reflection coefficient $|X_3|$ of the reflected SV-type

Table 1 Numerical values of the material constants

Symbol	Value	Unit	Symbol	Value	Unit
λ	7.76×10^{10}	N/m^2	μ	3.86×10^{10}	N/m^2
T_0	293	K	ρ	8954	kg/m^3
C_e	383.1	m^2/K	K_T	386	N/K s
α_T	383.1	/K	ε	0.0168	

wave first increases in the range $0\,\text{deg} \leq \theta_0 \leq 50\,\text{deg}$ and then decreases for $50\,\text{deg} \leq \theta_0 \leq 90\,\text{deg}$ for each τ. It is maximum at $\theta_0 = 50\,\text{deg}$ and vanishes at $\theta_0 = 0\,\text{deg}$ and $90\,\text{deg}$.

The key point, noticed from the Figs. 2(*a*)–2(*c*), is that while no significant effects of the delay time factor on the variations of $|X_1|$ and $|X_3|$ can be seen, only significant influences of τ can be seen markedly on the variation of $|X_2|$. This is most probably due to the following mechanism: as shown in Eq. (8) or (9), the MDD are introduced directly into the heat conduction equation instead of the constitutive equation to characterize the effects of the delay time parameter on the reflection coefficients of the various reflected waves, which in turn leads to the consequence that the delay time parameter barely influences the reflection coefficient, $|X_2|$ of the reflected qT-wave.

Figure 3 depicts the effect of the Poison's ratio σ on the variation of the moduli of the energy ratios $E_j\,(j = 1, 2, 3)$ with θ_0. We find that the pattern of each of $|E_j|$ with θ_0 is qualitatively similar to the pattern of the corresponding reflection coefficient (Supplementary Fig. 2 is available on the ASME Digital Collection), which is quite appealing as the energy ratios are proportional to the square of corresponding reflection coefficients at each θ_0. It is appeared from these figures that the maximum energy are carried along the reflected qP-wave and SV-type wave as the magnitude of E_2 is very small as compared to the others. It is also evident that the moduli of E_1 and E_2 increase and the $|E_3|$ decreases with an increase in the values of σ.

In order to validate the energy balance law at the surface $z = 0$, the energy ratios $|E_j|$ and their sum have been plotted for different θ_0 in Fig. 4(*a*). Since the absolute value of X_2 is found to be very small in comparing to the others, the corresponding energy ratio E_2 is also very small in the entire range of θ_0. So, $|E_2|$ is plotted after mounting up its original value by 10^5. It is observed that the sum $|E_1 + E_2 + E_3|$ keeps unity nearly at each θ_0, which verifies that the energy balance law at $z = 0$ is satisfied. However, Fig. 4(*b*) reveals a smaller deviation from unity of the energy conservation index ($|E_1 + E_2 + E_3|$), which is attributed to the loss of numerical precision. The approximate satisfaction of the energy balance law validates the present numerical results to a large extent.

Figure 5 is drawn in order to compare V_j and Q_j for the MDD, LS and the coupled thermoelasticity (CT) [40] theories. It is observed from Figs. 5(*a*) and 5(*b*) that the values of V_j for CT theory are found to be larger while the value of V_j are found to be smaller for LS theory. Similar patterns are noticed for the corresponding attenuation coefficients in Figs. 5(*c*) and 5(*d*) for all the theories. It is also clear from the graphs that the phase speeds and the attenuation coefficients of the qP- and qT-waves, respectively, reveal qualitatively similar nature for all the theories considered; however, dissimilarity lies on the ground of numerical values.

Supplementary Fig. 1 is available in the Supplemental Materials on the ASME Digital Collection reveals the profiles of $|X_j|$ with θ_0 for three different kernel function $K(t - \xi)$ when $\tau = 0.05$. It is evident from these figures that the qualitative behaviors of the reflection coefficients, $|X_j|$ are similar to those presented in Fig. 2, respectively. Supplementary Fig. 1 is available on the ASME Digital Collection. The key point, noticed from Supplementary Figs. 1(*a*)–1(*c*), is that while no significant effects of the kernel function on the variations of $|X_1|$ and $|X_3|$ can be seen, only significant influences of $K(t - \xi)$ can be seen markedly on the variation of $|X_2|$. The possible reason is explained in Fig. 2.

The effects of Poison's ratio (σ) on the magnitudes of X_j are depicted in Supplementary Fig. 2 is available on the ASME Digital Collection. In this purpose, we choose three values of σ as 0.34, 0.35, and 0.36 when $K(t, \xi) = 1 - (t - \xi)/\tau$, $\tau = 0.05$, $\varepsilon = 0.0168$, respectively. These figures express that σ affects prominently on each of the reflection coefficient $|X_j|$. While σ has an increasing effect on the variations of $|X_1|$ and $|X_2|$, it acts to decrease $|X_3|$. Supplementary Fig. 2 is available on the ASME Digital Collection.

Supplementary Fig. 3 is available on the ASME Digital Collection is drawn to show the influence of the thermomechanical coupling parameter (ε) on the variations of $|X_j|$ at fixed $K(t, \xi) = 1 - (t - \xi)/\tau$, $\tau = 0.05$. Here, we take three values of ε as 0, 0.0168 and 0.0336. We see from these figures that the absolute values of X_1 and X_2 have large values for large ε, meaning it has an increasing effect on $|X_1|$ and $|X_2|$ at each angle of incidence, while it has an decreasing effect on $|X_3|$. We can also observe that the influence of ε on $|X_1|$ and $|X_2|$ is very small as compared to the influence of ε on $|X_3|$. Another interesting fact is depicted in Supplementary Fig. 3(*b*) is available on the ASME Digital Collection that the reflection coefficient $|X_2|$ of the reflected qT-wave vanishes at each angle θ_0 for $\varepsilon = 0$, which is in complement agreement with our analytical results obtained in Sec. 5. Supplementary Fig. 3 is available on the ASME Digital Collection.

The dependency of the phase speeds V_j and the corresponding attenuation coefficients $Q_j\,(j = 1, 2)$ of the qP- and qT-waves on the angular frequency ω for the range $(1 \leq \omega \leq 10)$ is expressed in Supplementary Figs. 4 and 5 are available on the ASME Digital Collection, respectively, with the variations of τ and $K(t, \xi)$. Supplementary Figs. 4(*a*) and 4(*b*) on the ASME Digital Collection depict that $V_1 < V_2$ in the entire range of ω. The phase speed V_1 is decreasing while V_2 increases with increasing ω for all the values of τ. Supplementary Figs. 4(*c*) and 4(*d*) are on the ASME Digital Collection exhibit that the qP-wave is less attenuated than qT-wave. Supplementary Fig. 5 on the ASME Digital Collection reveals that the effect of $K(t, \xi)$ on V_j and Q_j is qualitatively similar to the effect of τ. From all these figures, it appears that both of the qP- and qT-waves are dispersive in nature as well as attenuated which agree with our analytical results discussed in Sec. 4. Supplementary Figs. 4 and 5 on the ASME Digital Collection.

8 Conclusion

The following points can be concluded according to the analysis above:

(1) The reflection coefficients and the corresponding energy ratios depend on the angle of incidence, Poison's ratio, and the thermoelastic coupling parameter.
(2) The time-delay and the kernel function have no significant effect on the reflection coefficients of the reflected qP- and SV-type waves, whereas these quantity reveals a significant effect on the reflection coefficient of the reflected qT-wave.
(3) The Poison's ratio has a prominent effect on the reflection coefficients and the corresponding energy ratios. It shows no effect on the phase speeds and the attenuation coefficients.
(4) The thermoelastic coupling parameter plays a significant role in the behavior of all the reflection coefficients and hence on the corresponding energy ratios also. The reflection coefficient of the reflected qT-wave is highly influenced by the thermoelastic coupling parameter as compared to the others two.
(5) The time-delay and the kernel function reveal a strong effect on the phase speeds and the attenuation coefficients of the qP- and qT-waves. The phase speed and the

attenuation coefficient of the SV-type wave are independent of the time-delay and the kernel function.

(6) We hope that our present theoretical results may provide some useful information for experimental scientists, researchers, and seismologists working on wave propagation problems in thermoelastic solid.

References

[1] Mainardi, F., 2010, *Fractional Calculus and Waves in Linear Viscoelasticity*, Imperial College Press, London.

[2] Diethelm, K., 2010, *Analysis of Fractional Differential Equation: An Application Oriented Exposition Using Differential Operators of Caputo Type*, Springer, Berlin.

[3] Wang, J. L., and Li, H. F., 2011, "Surpassing the Fractional Derivative: Concept of the Memory-Dependent Derivative," Comput. Math. Appl., **62**(3), pp. 1562–1567.

[4] Cattaneo, C., 1958, "Sur Une Forme de l'equation de la Chaleur Eliminant le Paradoxe D'une Propagation Instantanee," C. R. Acad. Sci., **247**, pp. 431–433.

[5] Green, A. E., and Naghdi, P. M., 1991, "A Re-Examination of the Basic Postulates of Thermomechanics," Proc. R. Soc. London Ser. A, **432**(1885), pp. 171–194.

[6] Lord, H. W., and Shulman, Y., 1967, "A Generalized Dynamical Theory of Thermoelasticity," J. Mech. Phys. Solids, **15**(5), pp. 299–309.

[7] Green, A. E., and Lindsay, K. A., 1972, "Thermoelasticity," J. Elasticity, **2**(1), pp. 1–7.

[8] Green, A. E., and Naghdi, P. M., 1992, "On Undamped Heat Waves in an Elastic Solid," J. Therm. Stress., **15**(2), pp. 253–264.

[9] Green, A. E., and Naghdi, P. M., 1993, "Thermoelasticity Without Energy Dissipation," J. Elasticity, **31**(3), pp. 189–208.

[10] Sherief, H. H., El-Sayed, A., and El-Latief, A., 2010, "Fractional Order Theory of Thermoelasticity," Int. J. Solids Struct., **47**(2), pp. 269–275.

[11] Youssef, H., 2010, "Theory of Fractional Order Generalized Thermoelasticity," ASME J. Heat Transfer, **132**(6), p. 061301.

[12] Ezzat, M. A., and Fayik, M. A., 2011, "Fractional Order Theory of Thermoelastic Diffusion," J. Therm. Stress., **34**(8), pp. 851–872.

[13] Yu, Y. J., Hu, W., and Tian, X. G., 2014, "A Novel Generalized Thermoelasticity Model Based on Memory-Dependent Derivative," Int. J. Eng. Sci., **81**, pp. 123–134.

[14] Ezzat, M. A., El-Karamany, A. S., and El-Bary, A. A., 2014, "Generalized Thermo-Viscoelasticity With Memory-Dependent Derivatives," Int. J. Mech. Sci., **89**, pp. 470–475.

[15] Ezzat, M. A., El-Karamany, A. S., and El-Bary, A. A., 2015, "A Novel Magneto-Thermoelasticity Theory With Memory-Dependent Derivative," J. Electromagn. Wave, **29**(8), pp. 1018–1031.

[16] Ezzat, M. A., El-Karamany, A. S., and El-Bary, A. A., 2016, "Modeling of Memory-Dependent Derivatives in Generalized Thermoelasticity," Eur. Phys. J. Plus, **131**(10), pp. 131–372.

[17] Lotfy, K., and Sarkar, N., 2017, "Memory-Dependent Derivatives for Photothermal Semiconducting Medium in Generalized Thermoelasticity With Two-Temperature," Mech. Time-Depend. Mater., **21**, pp. 15–30.

[18] Sarkar, N., Ghosh, D., and Lahiri, A., 2019, "A Two-Dimensional Magneto-Thermoelastic Problem Based on a New Two-Temperature Generalized Thermoelasticity Model With Memory-Dependent Derivative," Mech. Adv. Mater. Struct., **26**(11), pp. 957–966.

[19] Sarkar, N., and Mondal, S., 2019, "Transient Responses in a Two-Temperature Thermoelastic Infinite Medium Having Cylindrical Cavity Due to Moving Heat Source With Memory-Dependent Derivative," ZAMM-Z. Angew. Math. Mech., **99**(6), p. e201800343.

[20] Nayfeh, A. H., and Nemat-Nasser, S., 1972, "Electromagneto-Thermoelastic Plane Waves in Solids With Thermal Relaxation," ASME J. Appl. Mech., **39**(1), pp. 108–113.

[21] Agarwal, V. K., 1979, "On Electromagneto-Thermoelastic Plane Waves," Acta Mech., **34**(3–4), pp. 181–191.

[22] Roychoudhuri, S. K., 1985, "Effects of Rotation and Relaxation Times on Plane Waves in Generalized Thermoelasticity," J. Elasticity, **15**, pp. 59–68.

[23] Sinha, S. B., and Elsibai, K. A., 1996, "Reflection of Thermoelastic Waves at a Solid Half-Space With Two Relaxation Times," J. Therm. Stress., **19**, pp. 763–777.

[24] Chandrasekharaiah, D. S., 1996, "Thermoelastic Plane Waves Without Energy Dissipation," Mech. Res. Commun., **23**(5), pp. 549–555.

[25] Roychoudhuri, S. K., and Mukhopadhyay, S., 2000, "Effect of Rotation and Relaxation Times on Plane Waves in Generalized Thermo-Visco-Elasticity," Int. J. Math. Math. Sci., **23**(7), pp. 497–505.

[26] Sharma, J. N., Kumar, V., and Chand, D., 2003, "Reflection of Generalized Thermoelastic Waves From the Boundary of a Half Space," J. Therm. Stress., **26**(10), pp. 925–942.

[27] Das, N. C., Lahiri, A., Sarkar, S., and Basu, S., 2008, "Reflection of Generalized Thermoelastic Waves From Isothermal and Insulated Boundaries of a Half Space," Comput. Math. Appl., **56**(11), pp. 2795–2805.

[28] Othman, M. I. A., and Song, Y., 2008, "Reflection of Magneto-Thermoelastic Waves With Two Relaxation Times and Temperature Dependent Elastic Moduli," Appl. Math. Model., **32**(4), pp. 483–500.

[29] Sharma, J. N., Grover, D., and Kaur, D., 2011, "Mathematical Modelling and Analysis of Bulk Waves in Rotating Generalized Thermoelastic Media With Voids," Appl. Math. Model., **35**(7), pp. 3396–3407.

[30] Allam, M. N. M., Rida, S. Z., Abo-Dahab, S. M., Mohamed, R. A., and Kilany, A. A., 2014, "GL Model on Reflection of P and SV-Waves From the Free Surface of Thermoelastic Diffusion Solid Under Influence of the Electromagnetic Field and Initial Stress," J. Therm. Stress., **37**(4), pp. 471–487.

[31] Biswas, S., and Sarkar, N., 2018, "Fundamental Solution of the Steady Oscillations Equations in Porous Thermoelastic Medium With Dual-Phase-Lag Model," Mech. Mater., **126**, pp. 140–147.

[32] Li, Y., Wang, W., Wei, P., and Wang, C., 2018, "Reflection and Transmission of Elastic Waves at an Interface With Consideration of Couple Stress and Thermal Wave Effects," Meccanica, **53**(11–12), pp. 2921–2938.

[33] Sarkar, N., and Tomar, S. K., 2019, "Plane Waves in Nonlocal Thermoelastic solid With Voids," J. Therm. Stress., **42**(5), pp. 580–606.

[34] Mondal, S., Sarkar, N., and Sarkar, N., 2019, "Waves in Dual-Phase-Lag Thermoelastic Materials With Voids Based on Eringen's Nonlocal Elasticity," J. Therm. Stress., **42**(8), pp. 1035–1050.

[35] Das, N., Sarkar, N., and Lahiri, A., 2019, "Reflection of Plane Waves From the Stress-Free Isothermal and Insulated Boundaries of a Nonlocal Thermoelastic Solid," Appl. Math. Model., **73**, pp. 526–544.

[36] Sarkar, N., De, S., and Sarkar, N., 2019, "Memory Response in Plane Wave Reflection in Generalized Magneto-Thermoelasticity," J. Electromagn. Wave, **33**(10), pp. 1354–1374.

[37] Sarkar, N., De, S., and Sarkar, N., 2019, "Reflection of Thermoelastic Waves From the Isothermal Boundary of a Solid Half-Space Under Memory-Dependent Heat Transfer," Wave Random Complex, epub.

[38] Achenbach, J. D., 1976, *Wave Propagation in Elastic Solids*, North-Holland, New York.

[39] Li, Y., Li, L., Wei, P., and Wang, C., 2018, "Reflection and Refraction of Thermoelastic Waves at an Interface of Two Couple-Stress Solids Based on Lord-Shulman Thermoelastic Theory," Appl. Math. Model., **55**, pp. 536–550.

[40] Biot, M., 1956, "Thermoelasticity and Irreversible Thermodynamics," J. Appl. Phys., **27**(3), pp. 240–53.